

Stress-Energy Tensor Induced by Bulk Dirac Spinor in Randall-Sundrum Model

Shu-heng Shao^{1,3,*}, Pisin Chen^{1,2,3,4,†} and Je-An Gu^{3‡}

1. Department of Physics, National Taiwan University, Taipei 10617, Taiwan, R.O.C.

2. Graduate Institute of Astrophysics, National Taiwan University, Taipei 10617, Taiwan, R.O.C.

3. Leung Center for Cosmology and Particle Astrophysics,
National Taiwan University, Taipei 10617, Taiwan, R.O.C.

4. Kavli Institute for Particle Astrophysics and Cosmology,
SLAC National Accelerator Laboratory, Menlo Park, CA 94025, U.S.A.

(Dated: October 22, 2022)

Motivated by the possible extension into a supersymmetric Randall-Sundrum (RS) model, we investigate the properties of the vacuum expectation value (VEV) of the stress-energy tensor for a quantized bulk Dirac spinor field in the RS geometry and compare it with that for a real scalar field. This is carried out via the Green function method based on first principles without invoking the degeneracy factor, whose validity in a warp geometry is *a priori* unassured. In addition, we investigate the local behavior of the Casimir energy near the two branes. One salient feature we found is that the stress-energy tensor remains finite towards the Planck (hidden) brane yet diverges in the vicinity of the TeV (visible) brane. We discuss the implications of this “one-sided” surface divergence.

PACS numbers: 04.50.-h, 04.62.+v, 11.10.Kk, 11.25.-w, 11.30.Pb

I. INTRODUCTION

The hierarchy between the Planck scale, $M_{Pl} \sim 10^{19}$ GeV, and the standard model (SM) scale, $M_{SM} \sim 1$ TeV, has been a long-standing problem in high energy physics. In the past decade, there have been two popular solutions to the hierarchy problems: the Arkani-Hamed-Dimopoulos-Dvali (ADD) model [1] and the Randall-Sundrum (RS) model [2]. Both models invoke extra dimensions and the brane-world scenario. The weakness of gravity is associated with the largeness of the extra dimension in the case of ADD, while in RS it is due to the exponential warpage of the extra dimension. In this paper we shall only focus our attention on the latter. In the RS model, two flat, parallel 3-branes are located at two fixed points on a S^1/Z_2 orbifold. The metric of RS reads:

$$ds^2 = e^{-2\sigma(y)} \eta_{\mu\nu} dx^\mu dx^\nu + dy^2. \quad (1)$$

where R is the radius of the orbifold and y is the extra dimension coordinate ranging from $-\pi R$ to πR and $\sigma(y) = k|y|$. We adopt the convention $\eta_{\mu\nu} = \text{diag}(-1, 1, 1, 1)$. The brane located at $y = 0$ is called the hidden brane and that at $y = \pi R$ is the visible brane, on which the familiar SM fields reside. Under this construction, the hierarchy problem is naturally solved via the warp factor $e^{-k\pi R}$ along the extra dimension, generating a large hierarchy without requiring large extra dimensions. Specifically, with the choice of $kR \simeq 12$, the TeV scale at the visible brane can be descended from the Planck scale at the hidden brane.

With the introduction of a finite separation between the two branes in the extra dimension, any field in the bulk should induce a Casimir energy. This provides a possible resolution to the smallness problem of the cosmological constant when connected with the observed dark energy[3, 4, 5]. The Casimir effect in RS model generated by scalar fields has been studied in details by many authors[6, 7, 8, 9]. In [6], in particular, a detailed analysis of the *local* Casimir energy, or to be more specific, the vacuum expectation value (VEV) of stress-energy tensor, is given, in order to test the self-consistency of the model. It should be noted, as was pointed out by the authors of [6], however, that some conclusions made therein might not hold in a supersymmetric RS model, where the fermionic contribution is expected to exactly cancel its superpartner counterpart yet its local behavior has never been explicitly investigated. It is thus desirable to investigate the effect of the Casimir energy induced by the fermion field in the bulk.

With regard to the fermionic Casimir effect in RS geometry, some authors obtained the result by multiplying a degeneracy factor to that of the scalar field[10, 12]. In such an approach, calculations are performed via the mode summation method. We note that while such a transcription from the scalar field Casimir energy to that of the spinor field in a flat spacetime geometry is clear, that for the curved spacetime is not as transparent. This is mainly because the reduction from the Dirac equation to the Klein-Gordon equation in flat spacetime is unambiguous, whereas the similar procedure in the curved spacetime would induce a curvature coupling term[11]:

$$(-\nabla^2 + m_\psi^2 + \frac{1}{4}\hat{R})\psi = 0, \quad (2)$$

where ψ is the fermion field, \hat{R} is the Ricci scalar and m_ψ is the mass of the fermion. On the other hand, for

*Electronic address: b95202055@ntu.edu.tw

†Electronic address: pisinchen@phys.ntu.edu.tw

‡Electronic address: jagu@ntu.edu.tw

a scalar field ϕ in the curved spacetime, the equation of motion reads:

$$(-\nabla^2 + m_\phi^2 + \xi \hat{R})\phi = 0. \quad (3)$$

The ambiguity arises because the coupling parameter ξ between the scalar field and the curvature is generally not restricted to $\frac{1}{4}$, but as a free input to the theory. This motivates us to calculate the Casimir energy via the Green function method where the stress-energy tensor can be derived explicitly without resorting to the degeneracy factor.

We note that the vacuum energy arising from the fermion field in RS model has been fully discussed by Toms and coworkers [13][14] by computing the lowest order quantum corrections to the effective action. This approach can only provide the global properties of the vacuum energy and important local behavior might be overlooked. With the interest to fully understand the nature of the Casimir energy in the RS brane world, we find it desirable to directly compute the VEV for the stress-energy tensor, so as to compare it with that induced by the scalar field explicitly in the context of a SUSY system.

II. BASIC SETUP

Let us first distinguish two sets of labels in our metric:

$$ds^2 = g_{MN} dx^M dx^N = e^{-2\sigma(y)} \eta_{\mu\nu} dx^\mu dx^\nu + dy^2, \quad (4)$$

where the capital Latin labels denote the (4+1)-dimensional quantities: $M = 0, 1, 2, 3, 5$, so that $x^5 = y$, whereas $\mu = 0, 1, \dots, 3$. Then we write down the action for a Dirac spinor in the bulk with mass $m_\Psi = c\sigma'$ [15][17][18]:

$$S = \int d^4x \int dy \sqrt{-g} \left(i\bar{\Psi} \gamma^M D_M \Psi - m_\Psi \bar{\Psi} \Psi \right), \quad (5)$$

where $g = \det(g_{MN})$. The gamma matrices, γ^M are defined in curved spacetime as $\gamma^M = e_\alpha^M \gamma^\alpha$, where $e_\alpha^M = \text{diag}(e^\sigma, e^\sigma, e^\sigma, e^\sigma, 1)$ is the inverse vierbein and $\gamma^\alpha = (\gamma^\alpha, i\gamma^5)$ are the gamma matrices in flat spacetime, and $D_M = \partial_M + \Gamma_M$ is the covariant derivative in curved spacetime. With the metric defined in (4), we have

$$\Gamma_\mu = -\frac{i}{2} \sigma' e_{\beta\mu} \gamma^5 \gamma^\beta, \quad \Gamma_5 = 0. \quad (6)$$

It should be noted that the equation of motion derived from (5) with $m_\Psi = 0$ is automatically conformally covariant under proper choice of boundary condition, without the need for an additional conformal coupling term[19].

Given the Z_2 transformation for Dirac fermion: $\Psi(-y) = \pm \gamma^5 \Psi(y)$, it can be seen that $\bar{\Psi} \Psi$ is odd under Z_2 transformation. This implies that m_Ψ must also be odd under Z_2 transformation in order to preserve the

Z_2 symmetry of the Dirac equation. Therefore, m_Ψ can be parametrized as[15]

$$m_\Psi = c\sigma' = ck\epsilon(y). \quad (7)$$

where $\epsilon(y)$ is defined as being 1(-1) for positive(negative) y .

The stress-energy tensor related to the above action is given by

$$T_{MN} = i\bar{\Psi} \gamma_{(M} D_{N)} \Psi - g_{MN} L, \quad (8)$$

where the second term that involves the Lagrangian does not contribute to VEV by virtue of the equation of motion, and will be neglected in the following calculation.

III. COMPUTATION OF THE GREEN FUNCTION

In order to obtain the VEV of stress-energy tensor, we first calculate the Green function $G(x^M, x'^M)$ for the field, then express $\langle T_{MN} \rangle$ in terms of the Green function. The Green function by definition satisfies the field equation

$$(i\gamma^M D_M - m_\Psi)G(x^M, x'^M) = \frac{1}{\sqrt{-g}} \delta(x^M - x'^M). \quad (9)$$

To eliminate the dependence on the coordinates of x^μ , we perform a 4-dimensional Fourier transform on the Green function

$$G(x^M, x'^M) = \int \frac{d^3\vec{p}}{(2\pi)^3} \int \frac{d\omega}{2\pi} e^{i\vec{p}\cdot(\vec{x}-\vec{x}')} e^{-i\omega(t-t')} G_p(y, y'). \quad (10)$$

Then (9) becomes

$$[-\gamma^\mu p_\mu - \gamma^5 \partial_5 - m_\Psi] \tilde{G}_p(y, y') = e^{2\sigma} \delta(y - y') I_{4 \times 4}. \quad (11)$$

where $\tilde{G}_p(y, y') \equiv e^{-2\sigma} G_p(y, y')$.

We further write the Green function as

$$\tilde{G}_p(y, y') = \begin{pmatrix} f_1 & f_2 \\ g_1 & g_2 \end{pmatrix}. \quad (12)$$

where f_1, f_2, g_1, g_2 are 4×4 matrices. Put this back into (11), we arrive at the following 4 equations for the 4 elements of the Green function:

$$-\partial_5 f_1 + ck f_1 + e^\sigma \sigma^\alpha p_\alpha g_1 = -e^{2\sigma} \delta(y - y') I_{2 \times 2}, \quad (13a)$$

$$e^\sigma \bar{\sigma}^\alpha p_\alpha f_1 + \partial_5 g_1 + ck g_1 = 0, \quad (13b)$$

$$-\partial_5 f_2 + ck f_2 + e^\sigma \sigma^\alpha p_\alpha g_2 = 0, \quad (13c)$$

$$e^\sigma \bar{\sigma}^\alpha p_\alpha f_2 + \partial_5 g_2 + ck g_2 = -e^{2\sigma} \delta(y - y') I_{2 \times 2}. \quad (13d)$$

If we neglect the Dirac delta functions on the right hand sides of (13a)~ (13d), the solutions are[15]

$$f_i(y) = \frac{e^{\sigma/2}}{N_i} [J_{c-\frac{1}{2}}(mz) + b_i H_{c-\frac{1}{2}}^1(mz)], \quad (14)$$

$$g_i(y) = \frac{e^{\sigma/2}}{N_i} [J_{c+\frac{1}{2}}(mz) + d_i H_{c+\frac{1}{2}}^1(mz)]. \quad (15)$$

where $m \equiv \sqrt{-p^2}$ is the Kaluza-Klein mass, $z \equiv e^\sigma/k$, $i = 1, 2$. N_i and b_i are the coefficients to be determined by normalization and by our choice of the boundary condition (BC). Generally, there are two distinct classes of BCs for Dirac fermion, the untwisted and the twisted BC[15][16]. These BCs are defined as follows.

Untwisted:

$$\begin{aligned} \Psi_L|_{0=0}, & \quad \Psi_L|_{\pi R}=0, \\ (\partial_5 + ck)\Psi_R|_{0=0}, & \quad (\partial_5 + ck)\Psi_R|_{\pi R}=0. \end{aligned} \quad (16a)$$

Twisted:

$$\begin{aligned} \Psi_L|_{0=0}, & \quad (\partial_5 - ck)\Psi_L|_{\pi R}=0, \\ (\partial_5 + ck)\Psi_R|_{0=0}, & \quad \Psi_R|_{\pi R}=0, \end{aligned} \quad (16b)$$

where $\Psi_{L,R} = [(1 \mp \gamma^5)/2]\Psi$. We'll deal with both cases.

A. The Untwisted BC

For later convenience, we introduce the following four functions to represent different combinations of the special functions that appeared in (14) or (15)

$$\eta(y) \equiv e^{\frac{\sigma}{2}} [J_{c-\frac{1}{2}}(mz) + b H_{c-\frac{1}{2}}^1(mz)], \quad (17)$$

$$\dot{\eta}(y) \equiv e^{\frac{\sigma}{2}} [J_{c-\frac{1}{2}}(mz) + \dot{b} H_{c-\frac{1}{2}}^1(mz)], \quad (18)$$

$$\lambda(y) \equiv -e^{\frac{\sigma}{2}} [J_{c+\frac{1}{2}}(mz) + b H_{c+\frac{1}{2}}^1(mz)], \quad (19)$$

$$\dot{\lambda}(y) \equiv -e^{\frac{\sigma}{2}} [J_{c+\frac{1}{2}}(mz) + \dot{b} H_{c+\frac{1}{2}}^1(mz)], \quad (20)$$

where

$$b = -\frac{J_{c-\frac{1}{2}}(\frac{m}{k})}{H_{c-\frac{1}{2}}^1(\frac{m}{k})}, \quad (21)$$

$$\dot{b} = -\frac{J_{c-\frac{1}{2}}(\frac{me^{\pi k R}}{k})}{H_{c-\frac{1}{2}}^1(\frac{me^{\pi k R}}{k})}. \quad (22)$$

In terms of these new functions, the untwisted BCs become

$$\begin{aligned} \eta|_{0=0}, & \quad \dot{\eta}|_{\pi R}=0, \\ (\partial_5 + ck)\lambda|_{0=0}, & \quad (\partial_5 + ck)\dot{\lambda}|_{\pi R}=0. \end{aligned} \quad (23)$$

We first deal with f_1 and g_1 . Under the above definitions, f_1 and g_1 can be expressed as

$$f_1(y, y') = \begin{cases} \begin{pmatrix} \alpha & \gamma \\ \bar{\alpha} & \bar{\gamma} \end{pmatrix} \eta(y), & \text{if } y < y' \\ \begin{pmatrix} \acute{\alpha} & \acute{\gamma} \\ \acute{\bar{\alpha}} & \acute{\bar{\gamma}} \end{pmatrix} \dot{\eta}(y), & \text{if } y > y' \end{cases} \quad (24)$$

$$g_1(y, y') = \begin{cases} \begin{pmatrix} \beta & \delta \\ \bar{\beta} & \bar{\delta} \end{pmatrix} \lambda(y), & \text{if } y < y' \\ \begin{pmatrix} \acute{\beta} & \acute{\delta} \\ \acute{\bar{\beta}} & \acute{\bar{\delta}} \end{pmatrix} \dot{\lambda}(y), & \text{if } y > y' \end{cases} \quad (25)$$

All the parameters in the above matrices are determined by (13a) and (13b), from which we get

$$g_1|_{y=y'^+} - g_1|_{y=y'^-} = 0, \quad (26)$$

$$f_1|_{y=y'^+} - f_1|_{y=y'^-} = e^{2\sigma(y')} I_{2 \times 2}, \quad (27)$$

$$-\partial_5 f_1 + ck f_1 + e^\sigma \sigma^\alpha p_\alpha g_1 = 0. \quad (28)$$

These together constitute 16 linear equations for 16 unknowns. Here we solved it by the help of `Mathematica 7.0`:

$$f_1(y, y') = \begin{cases} -I_{2 \times 2} e^{2\sigma(y')} \frac{\dot{\lambda}(y')}{S} \eta(y), & \text{if } y < y' \\ -I_{2 \times 2} e^{2\sigma(y')} \frac{\lambda(y')}{S} \dot{\eta}(y), & \text{if } y > y' \end{cases} \quad (29)$$

$$g_1(y, y') = \begin{cases} -\bar{\sigma}^\alpha p_\alpha e^{2\sigma(y')} \frac{\dot{\lambda}(y')}{mS} \lambda(y), & \text{if } y < y' \\ -\bar{\sigma}^\alpha p_\alpha e^{2\sigma(y')} \frac{\lambda(y')}{mS} \dot{\lambda}(y), & \text{if } y > y' \end{cases} \quad (30)$$

where

$$S \equiv \dot{\lambda}\eta - \lambda\dot{\eta}|_{y'}. \quad (31)$$

The remaining two elements, f_2 and g_2 , can be obtained in a similar way

$$f_2(y, y') = \begin{cases} -\sigma^\alpha p_\alpha e^{2\sigma(y')} \frac{\dot{\eta}(y')}{mS} \eta(y), & \text{if } y < y' \\ -\sigma^\alpha p_\alpha e^{2\sigma(y')} \frac{\eta(y')}{mS} \dot{\eta}(y), & \text{if } y > y' \end{cases} \quad (32)$$

$$g_2(y, y') = \begin{cases} -I_{2 \times 2} e^{2\sigma(y')} \frac{\dot{\eta}(y')}{S} \lambda(y), & \text{if } y < y' \\ -I_{2 \times 2} e^{2\sigma(y')} \frac{\eta(y')}{S} \dot{\lambda}(y), & \text{if } y > y' \end{cases} \quad (33)$$

With (29), (30), (32), (33), we finish our calculation for the Green function subjected to the untwisted BC.

B. The Twisted BC

In order to fit the twisted BC (16b), we define additional two functions

$$\tilde{\eta}(y) \equiv -e^{\frac{\sigma}{2}} [J_{c+\frac{1}{2}}(mz) + \tilde{b} H_{c+\frac{1}{2}}^1(mz)], \quad (34)$$

$$\tilde{\lambda}(y) \equiv e^{\frac{\sigma}{2}} [J_{c-\frac{1}{2}}(mz) + \tilde{b} H_{c-\frac{1}{2}}^1(mz)], \quad (35)$$

where

$$\tilde{b} = -\frac{J_{c+\frac{1}{2}}\left(\frac{me^{\pi kR}}{k}\right)}{H_{c+\frac{1}{2}}^1\left(\frac{me^{\pi kR}}{k}\right)}, \quad (36)$$

so that

$$\tilde{\eta}|_{\pi R=0}, \quad (\partial_5 - ck)\tilde{\lambda}|_{\pi R=0}. \quad (37)$$

If we rewrite (24) and (25) with the replacements $\tilde{\eta} \rightarrow \tilde{\lambda}$ and $\tilde{\lambda} \rightarrow \tilde{\eta}$, the remaining calculations are completely identical to that of the untwisted case. The results are just the same as (29), (30), (32) and (33) with the above substitution.

IV. STRESS-ENERGY TENSOR

Now well-equipped with the exact form of the Green functions for both untwisted and twisted BCs, namely, (29)~(33), together with the definition (12), we are finally at a position to calculate the VEV of the stress-energy tensor. First, we make the identification

$$iG(x^M, x'^M) = \langle \Psi(x^M) \bar{\Psi}(x'^M) \rangle. \quad (38)$$

With this identification, we can replace any VEV involving the quadratic terms of the field by the Green function. We begin with the VEV of T_{00} in (8),

$$\begin{aligned} \langle T_{00} \rangle &= ie_{00} \langle \bar{\Psi} \gamma^0 D_0 \Psi \rangle \\ &= -ie^{-\sigma} [i\partial_0 \text{Tr}(\gamma^0 G)]_{x^M=x'^M}. \end{aligned} \quad (39)$$

In the second equality we have neglected the spin connection term Γ_0 in the covariant derivative D_0 , since it turns out to be a term independent of the mode, and thus can be omitted in the renormalization. Let us first deal with the untwisted BC. We perform a 4-dimensional Fourier transform on both sides of (39) and use (12) to obtain

$$\begin{aligned} \langle t_{00} \rangle &= -i\omega e^\sigma \text{Tr}(g_1 + f_2)|_{y=y'} \\ &= -2ie^{3\sigma} \frac{\omega^2}{m} \frac{\dot{\lambda}\lambda + \dot{\eta}\eta}{\dot{\lambda}\eta - \dot{\lambda}\dot{\eta}} \quad (\text{Untwisted BC}), \end{aligned} \quad (40)$$

where t_{00} is the 4-dimensional Fourier transformation of T_{00} . In a similar fashion, we obtain the other entries of the stress-energy and also those for the twisted BC as follows.

$$\begin{aligned} \langle T_{\mu\nu} \rangle &= \\ &\begin{cases} -2i\delta_{\mu\nu} e^{3\sigma} \int \frac{d^3\vec{p}}{(2\pi)^3} \int \frac{d\omega}{2\pi} \frac{(p^\mu)^2}{m} \frac{\dot{\lambda}\lambda + \dot{\eta}\eta}{\dot{\lambda}\eta - \dot{\lambda}\dot{\eta}}, & \text{untwisted} \\ -2i\delta_{\mu\nu} e^{3\sigma} \int \frac{d^3\vec{p}}{(2\pi)^3} \int \frac{d\omega}{2\pi} \frac{(p^\mu)^2}{m} \frac{\tilde{\eta}\lambda + \tilde{\lambda}\eta}{\tilde{\eta}\eta - \tilde{\lambda}\lambda}, & \text{twisted} \end{cases} \end{aligned} \quad (41)$$

$$\begin{aligned} \langle T_{yy} \rangle &= \\ &\begin{cases} -ie^{4\sigma} \int \frac{d^3\vec{p}}{(2\pi)^3} \int \frac{d\omega}{2\pi} \partial_5 \left(\frac{\dot{\lambda}\lambda + \dot{\eta}\eta}{\dot{\lambda}\eta - \dot{\lambda}\dot{\eta}} \right) |_{y=y'}, & \text{untwisted} \\ -ie^{4\sigma} \int \frac{d^3\vec{p}}{(2\pi)^3} \int \frac{d\omega}{2\pi} \partial_5 \left(\frac{\tilde{\eta}\lambda + \tilde{\lambda}\eta}{\tilde{\eta}\eta - \tilde{\lambda}\lambda} \right) |_{y=y'}, & \text{twisted} \end{cases} \end{aligned} \quad (42)$$

where $\delta_{\mu\nu} = \text{diag}(1, 1, 1, 1)$. This is our final expression for the stress-energy tensor. The integral cannot be expressed analytically for a general c , and suitable renormalization must be implemented. For the massless case, however, the results can be written in a concise way.

V. MASSLESS DIRAC FERMION

Now consider the simplest case: $c = 0$, in which all η and λ functions reduce to basic trigonometric functions, and (41) and (42) become

$$\begin{aligned} \langle T_{\mu\nu} \rangle &= \\ &\begin{cases} -2i\delta_{\mu\nu} e^{3\sigma} \int \frac{d^3\vec{p}}{(2\pi)^3} \int \frac{d\omega}{2\pi} \frac{(p^\mu)^2}{m} \cot\left[\frac{m}{k}(e^{\pi kR} - 1)\right], & \text{untwisted} \\ 2i\delta_{\mu\nu} e^{3\sigma} \int \frac{d^3\vec{p}}{(2\pi)^3} \int \frac{d\omega}{2\pi} \frac{(p^\mu)^2}{m} \tan\left[\frac{m}{k}(e^{\pi kR} - 1)\right], & \text{twisted} \end{cases} \end{aligned} \quad (43)$$

$$\begin{aligned} \langle T_{yy} \rangle &= \\ &\begin{cases} -2ie^{5\sigma} \int \frac{d^3\vec{p}}{(2\pi)^3} \int \frac{d\omega}{2\pi} m \cot\left[\frac{m}{k}(e^{\pi kR} - 1)\right], & \text{untwisted} \\ 2ie^{5\sigma} \int \frac{d^3\vec{p}}{(2\pi)^3} \int \frac{d\omega}{2\pi} m \tan\left[\frac{m}{k}(e^{\pi kR} - 1)\right], & \text{twisted} \end{cases} \end{aligned} \quad (44)$$

The integrations are best done by performing a Wick rotation

$$\omega \rightarrow ip^4, \quad m = \sqrt{\omega^2 - \vec{p}^2} \rightarrow ip. \quad (45)$$

Thus the stress-energy tensor is given by

$$\begin{aligned} \langle T_{\mu\nu} \rangle &= \\ &\begin{cases} -2\eta_{\mu\nu} e^{3\sigma} \int \frac{d^4 p}{(2\pi)^4} \frac{(p^\mu)^2}{p} \coth\left[\frac{p}{k}(e^{\pi kR} - 1)\right], & \text{untwisted} \\ -2\eta_{\mu\nu} e^{3\sigma} \int \frac{d^4 p}{(2\pi)^4} \frac{(p^\mu)^2}{p} \tanh\left[\frac{p}{k}(e^{\pi kR} - 1)\right], & \text{twisted} \end{cases} \end{aligned} \quad (46)$$

$$\begin{aligned} \langle T_{yy} \rangle &= \\ &\begin{cases} 2e^{5\sigma} \int \frac{d^4 p}{(2\pi)^4} p \coth\left[\frac{p}{k}(e^{\pi kR} - 1)\right], & \text{untwisted} \\ 2e^{5\sigma} \int \frac{d^4 p}{(2\pi)^4} p \tanh\left[\frac{p}{k}(e^{\pi kR} - 1)\right], & \text{twisted} \end{cases} \end{aligned} \quad (47)$$

The renormalization procedure for the integral is conventional, where one subtracts 1 from the coth or tanh function. The results read (for a more detailed calculation, see, for example, [6] or [20])

$$\begin{aligned} \langle T_{\mu\nu} \rangle_{\text{ren}} &= \\ &\begin{cases} -e^{3\sigma} \eta_{\mu\nu} 2^{-3} \pi^{-\frac{5}{2}} a^{-5} \Gamma\left(\frac{5}{2}\right) \zeta(5), & \text{untwisted} \\ \frac{15}{16} e^{3\sigma} \eta_{\mu\nu} 2^{-3} \pi^{-\frac{5}{2}} a^{-5} \Gamma\left(\frac{5}{2}\right) \zeta(5), & \text{twisted} \end{cases} \end{aligned} \quad (48)$$

$$\begin{aligned} \langle T_{yy} \rangle_{\text{ren}} &= \\ &\begin{cases} \frac{1}{2} e^{5\sigma} \pi^{-\frac{5}{2}} a^{-5} \Gamma\left(\frac{5}{2}\right) \zeta(5), & \text{untwisted} \\ -\frac{15}{32} e^{5\sigma} \pi^{-\frac{5}{2}} a^{-5} \Gamma\left(\frac{5}{2}\right) \zeta(5), & \text{twisted} \end{cases} \end{aligned} \quad (49)$$

where $a = (e^{\pi kR} - 1)/k$. Compare with the VEV of the stress-energy tensor for scalar fields given in [6], we conclude that

$$\langle T_{MN} \rangle_{\text{Dirac, untwisted}} = -4 \langle T_{MN} \rangle_{\text{real scalar}} \quad (50)$$

$$\langle T_{MN} \rangle_{\text{Dirac, twisted}} = \frac{15}{4} \langle T_{MN} \rangle_{\text{real scalar}} \quad (51)$$

The factor 4, as indicated in [10], accounts for the difference of the degrees of freedom between the Dirac spinor and the real scalar fields. The sign difference originates from the distinct natures of fermions and bosons. As for the factor 15/16 between the untwisted and the twisted results, it results from the difference in renormalization between the coth and the sinh functions.

VI. MASSIVE DIRAC FERMION

To extract useful information from the VEV of stress-energy tensor for a general mass c , we need to appeal to the numerical method. In this section, we will only focus on the numerical integration of the 00 component of $\langle T_{MN} \rangle$ for the *untwisted BC*, namely, (40). For later convenience, we denote

$$F(p, y; R) \equiv \frac{\dot{\lambda}\lambda + \dot{\eta}\eta}{\dot{\lambda}\eta - \lambda\dot{\eta}}. \quad (52)$$

Recall that R is the radius of the RS geometry. So our goal is to renormalize the integral

$$\langle T_{00} \rangle = iC \int_0^\infty dp p^4 F(ip, y; R), \quad (53)$$

with

$$C \equiv \frac{\pi^{-\frac{5}{2}} \Gamma(\frac{3}{2})}{4 \Gamma(3)} e^{3\sigma(y)}. \quad (54)$$

Note that the Wick rotation has been performed in the above expression.

While there is no ambiguity in the renormalization for the massless spinor field, care must be taken for the massive case. By definition, the Casimir energy is the *difference* between the vacuum energies with and without boundaries. That means we need to subtract (53) off the energy with no boundary present, i.e., with $R \rightarrow \infty$:

$$\langle T_{00} \rangle_{\text{ren}} = iC \int_0^\infty dp p^4 [F(ip, y; R) - \lim_{R \rightarrow \infty} F(ip, y; R)] \quad (55)$$

As a check, we take the $c = 0$ limit in the above equation and find

$$\langle T_{00} \rangle_{\text{ren}}(c = 0) \propto \int_0^\infty dp p^4 \left\{ \coth\left[\frac{p}{k}(e^{\pi k R} - 1)\right] - 1 \right\}, \quad (56)$$

which coincides with the renormalization given in the previous section.

Next we proceed with the massive case. To facilitate the computation, we expand $F(ip, y; R)$ and its limit to the first order in c . Since c represents the fermion mass in units of Planck mass, it is expected to be very small for a physical particle, thus ensuring the validity of our approximation. In addition, to make the computer run more effectively, we set $k = R = 1$ as in [6], although the more “realistic” value would be $kR \simeq 12$ with $k \simeq M_{Pl}$.

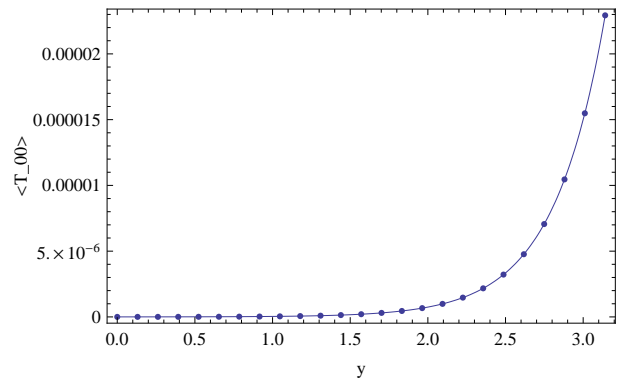


FIG. 1: The massless ($c=0$), untwisted BC case for $\langle T_{00} \rangle_{\text{ren}}$ in units of k^4 . The branes are located at $y = 0$ and $y = \pi$ and $kR = 1$. Note that the numerical value (points) agrees perfectly with the exact solution.

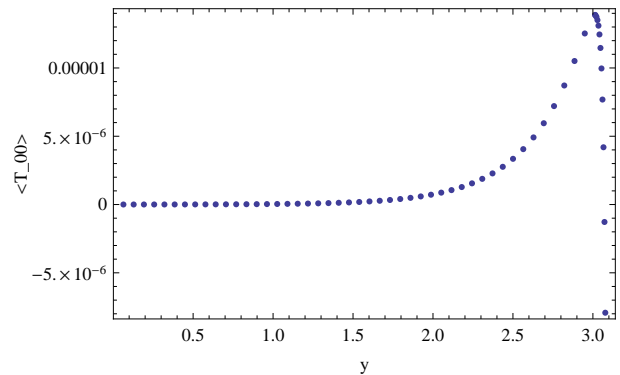


FIG. 2: The massive ($c = 10^{-4}$), untwisted BC case for $\langle T_{00} \rangle_{\text{ren}}$ in units of k^4 . The energy density diverges at the visible brane $y = \pi R$.

The results are given in Fig. 1 and Fig. 2. It can be seen that the energy density diverges to minus infinity near the visible brane $y = \pi R$. We’ll discuss this “one-sided” surface divergence in the following subsection.

A. “One-sided” Surface Divergence

In Ref.[22], the authors pointed out that the surface divergence is mainly contributed by the high wave number (momentum) modes in the Fourier transformation of $\langle T_{MN} \rangle$. Based on the same philosophy, we expand the integrand of (55) asymptotically in powers of p^{-n} and retain only the p^{-1} term, which dominates the integrand

for large p , i.e.,

$$\begin{aligned} \langle T_{00} \rangle_{\text{ren}} &\simeq C \int_0^\infty dp p^4 \left[\coth\left(\frac{\alpha-1}{k}\right)p - 1 \right] \\ &+ C \int_0^\infty dp p^4 \frac{c}{4z\alpha p} \left[\text{csch}\left(\frac{\alpha-1}{k}\right)p \right]^2 \left\{ (\alpha-1)2kz + \right. \\ &\left. \alpha e^{\frac{2p}{k}(kz-\alpha)} - \alpha e^{\frac{2p}{k}(2-\alpha-kz)} - 2\alpha \sinh\left[\frac{2p}{k}(kz-1)\right] \right\}, \end{aligned} \quad (57)$$

where $\alpha \equiv e^{\pi k R}$. The first term is just the result for massless fermion while the second term corresponds to the correction due to the fermion mass. Note that the mass correction term is proportional to c by virtue of the small mass expansion to the first order.

The expression remains complicated. However, since only the high wave number behavior concerns us, we isolate the dominating term by taking the large p limit again and find

$$\langle T_{00} \rangle_{\text{ren}} \sim C \int_0^\infty dp \frac{cp^3}{4z} \left[e^{\frac{2p}{k}(kz-2\alpha+1)} - e^{\frac{2p}{k}(kz-\alpha)} \right]. \quad (58)$$

Since $kz \equiv e^{ky}$ ranges from 1 to $\alpha = e^{\pi k R}$, we find the near-brane behaviors to be

$$\langle T_{00} \rangle_{\text{ren}}|_{y \rightarrow 0} \propto \frac{ce^{3ky}}{(y+2-2e^{\pi k R})^4}, \quad (59)$$

$$\langle T_{00} \rangle_{\text{ren}}|_{y \rightarrow \pi R} \propto \frac{ce^{3ky}}{(y-\pi R)^4}. \quad (60)$$

We observe that while the energy density diverges at the visible brane, it is *finite* at the hidden brane. This “one-sided” surface divergence agrees with our numerical result shown in Fig. 2. It should be noted that the divergence only disappears in the limit of $c = 0$, the massless and conformally symmetric case, which is consistent with our previous result.

The asymmetry aspect of the divergence lies in the fact that RS geometry by itself is not symmetric upon the exchange of the two branes. On the contrary, this symmetry breaking does not happen in the flat spacetime by virtue of the exchange symmetry between the two boundaries. That is, surface divergence occurs either on both or neither boundaries in the case of flat spacetime. Moreover, this asymmetry cannot be remedied by “pulling” $y = 0$ and “pushing” $y = \pi R$ brane to the minus or plus infinity simultaneously. Since RS geometry is an orbifold rather than a manifold with two branes as its boundaries, each of the two branes stands at its special position with respect to the Z_2 symmetry, and thus cannot be altered at will. The RS metric, being a solution to the Einstein equation, *must* take its two branes at $y = 0$ and $y = \pi R$, or at most up to a change of variable. The only thing we can alter is the radius R . In other words, the “one-sided” surface divergence is an inherent nature of RS geometry, independent of the technique of renormalization one adopts.

It should also be noted that the near-brane behavior given in (59) and (60) could *not* be reduced to the flat parallel plates result in (4+1) dimension, because the flat spacetime limit, i.e., the $k \rightarrow 0$ limit, in general does not commute with the $R \rightarrow \infty$ limit. To be more specific, there exists an ambiguity in taking the limit of $e^{\pi k R}$ in (40) for the massive case, while in contrast this can be performed unequivocally for the massless case in (46) and (47). That is, as an exception for the massless case, the $k \rightarrow 0$ limit correctly reduces (48) and (49) to the flat spacetime result by virtue of the compact, well-behaved expressions of the terms $\coth\left[\frac{p}{k}(e^{\pi k R} - 1)\right]$ and $\tanh\left[\frac{p}{k}(e^{\pi k R} - 1)\right]$ in (46) and (47). In contrast, no such package deal can be found for the massive case. The distinct outcomes of the massive and massless cases in taking the flat limit may be another evidence for the special role played by the conformal symmetry. It is known, for example, that the stress-energy tensor for a *canonical* scalar field is less well-behaved than that of the conformally coupled one with regard to the divergence near the boundaries. Similar situation occurs here. We found that the flat limit $k \rightarrow 0$ can only be achieved in the massless fermion case, which possesses the conformal symmetry.

With regard to the non-integrable divergence of the stress-energy tensor, the problem was solved by Kennedy, Critchley, and Dowker[23] for a scalar field in a static spacetime. The resolution lies in the renormalization of the bare surface gravitational action, which induces a delta function and that cancels exactly with the surface divergence. Since in our result the divergence appears only on the visible brane but not on the hidden one, the corresponding bare surface terms in the effective action are definitely not the same. It is thus intriguing to ask what roles do these brane terms play, and what is the physical implication of their difference.

VII. DISCUSSIONS

In flat spacetime, the one-loop correction to the effective action, and therefore the Casimir energy, of the massless Dirac spinor field can be obtained simply by multiplying a suitable degeneracy factor to that of the scalar field. In the case of curved spacetime, however, the above statement is not valid in general. In this paper, we provide a complete and straightforward derivation, using the Green function approach, of these degeneracy factors, which are -4 and $15/4$ for the untwisted and twisted BC, respectively, as expected. For a massive fermion, the exotic phenomenon of “one-sided” surface divergence occurs due to the nature of the RS geometry. To cure this non-integrability, an approach similar to that of Ref. [23] must be implemented where the surface terms are included.

On the other hand, this infinity might be originated from the unphysical nature of the boundary condition. This may suggest the necessity of including the finite thickness (of string length) of the 3-brane, in particular

the one we live on, in the treatment. Similar situation happens in the perfect conductor boundary condition for electromagnetic field [22, 24, 25], in which a strictly zero thickness boundary gives rise to a non-integrable divergence. For an imperfect conductor, such as a dielectric material, or a conductor with finite thickness, waves of sufficiently high frequency would penetrate into the material so that the precise location of the boundary would lose its meaning. Therefore, in reality, the divergence does not appear since the expression of the integrand is not universally applicable for all wave numbers. We wonder whether the finite thickness of the 3-brane would provide a similar remedy to this divergence problem.

We expect that the nature of the “one-sided” surface divergence to be a generic feature of the Casimir energy for all non-conformally symmetric fields in RS geometry, due to its lack of homogeneity. However, in Ref. [6] no such near-brane behavior was pointed out for the scalar field, possibly due to the different normalization scheme adopted by its authors. It would be interesting

to reexamine the local behavior for a massive scalar field, and compare it with that for a massive fermion given in this paper. Such an investigation becomes inevitable if one wishes to better understand the local behavior of the Casimir energy in a SUSY-RS scenario, such as one based on the hypermultiplet in [15].

Acknowledgments

We thank L. P. Teo (University of Malaysia) and P. M. Ho (NTU) for their useful suggestions and comments on the subject. We are also grateful to K.Y. Su, Y. D. Huang and C. I. Chiang for interesting and encouraging discussions. This research is supported by Taiwan National Science Council under Project No. NSC 97-2112-M-002-026-MY3 and by US Department of Energy under Contract No. DE-AC03-76SF00515.

-
- [1] N. Arkani-Hamed, S. Dimopoulos and G. Dvali, Phys. Lett. B **429**, 263 (1998).
 - [2] L. Randall and R. Sundrum, Phys. Rev. Lett. **83**, 3370 (1999).
 - [3] K. A. Milton, Grav. Cosmol. **9**, 66 (2003).
 - [4] P. Chen, Nucl. Phys. Proc. Suppl. **173**, S8 (2009); arXiv:hep-ph/0611378.
 - [5] P. Chen and Je-An Gu, Mod. Phys. Lett. **A22**, 1995 (2007).
 - [6] A. Knapman. and D. J. Toms, Phys. Rev. D **69**, 044023 (2004)
 - [7] A. A. Saharian, arXiv:hep-th/0312092v2
 - [8] M. Frank, I. Turan, L. Ziegler, Phys. Rev. D **76**, 015008 (2007)
 - [9] D. J. Toms, Phys. Lett. B **484** 2000 149
 - [10] E. Ponton, E. Poppitz, arXiv:hep-ph/0105021
 - [11] See, for example, I. I. Cotaescu, M. Visinescu, arXiv:hep-th/0411016v2
 - [12] R. Obousy, G. Cleavery, arXiv:0810.1096v2
 - [13] A. Flachi, I. G. Moss, D. J. Toms, arXiv:hep-th/0103138v2
 - [14] A. Flachi, I. G. Moss, D. J. Toms, Phys. Rev. D, **64**, 105029 (2001)
 - [15] T. Gherghetta, A. Pomarol, Nuclear Physics B **586** (2000) 141
 - [16] T. Gherghetta, A. Pomarol, Nuclear Physics B **602** (2001) 3
 - [17] Y. Grossman, M. Neubert, arXiv:hep-ph/9912408v3
 - [18] T. Gherghetta, arXiv:hep-ph/0601213v1
 - [19] See, e.g.: N. D. Birrell, P. C. W. Davies, *Quantum Fields in Curved Spacetime*, Cambridge University Press, 1982
 - [20] K. A. Milton, *The Casimir Effect: Physical Manifestations of Zero-Point Energy*, World Scientific, 2001
 - [21] G. N. Watson, *A Treatise on the Theory of Bessel Functions, Second Edition*, Cambridge University Press, 1995
 - [22] D. Deutsch and P. Candelas, Phys. Rev. D **20** (1979) 3063.
 - [23] G. Kennedy, R. Critchley and J. S. Dowker, Annals Phys. **125** (1980) 346.
 - [24] R. Balian and B. Duplantier, Ann. Phys. (N.Y.) **104** (1977), 330-335.
 - [25] R. Balian and B. Duplantier, Ann. Phys. (N.Y.) **112** (1978), 165-208.